Nuclear Data for Science and Technology (1988 MITO), 1045-1048, Copyright © 1988 JAERI.

CROSS SECTIONS AND PARTIAL KERMA FACTORS FOR ELASTIC AND INELASTIC NEUTRON SCATTERING FROM CARBON IN THE ENERGY RANGE 16.5 - 22.0 MeV.

N. Olsson, B. Trostell and E. Ramström,

Department of Neutron Research, Uppsala University,
S-61182 Nyköping, Sweden

Abstract: The Studsvik high resolution, low background time-of-flight facility has been used to obtain a comprehensive set of differential neutron scattering cross sections for carbon at the neutron energies 16.5, 17.6, 18.7, 19.8, 20.9, 21.6 and 22.0 MeV. Angular distributions in the range 10° - 160° have been measured for elastic scattering, and also for inelastic scattering from the levels at 4.44, 7.65 and 9.64 MeV. Angle integrated cross sections have been determined by fitting Legendre polynomial expansions to the differential data. Partial kerma factors for elastic and inelastic (4.44 MeV level) scattering have been deduced from these fits. Analyses in terms of the coupled-channels formalism for rotational nuclei have provided information for cross section and partial kerma factor calculations also outside the measured energy range, i.e. from 15 up to 40 MeV.

(elastic, inelastic, neutron scattering, carbon sample, fast neutrons, time-of-flight, coupled-channels analysis, partial kerma factors)

Introduction

Precise knowledge of neutron scattering cross sections and kerma factors for carbon is very important in many applications. One of these deals with neutron dose deposition in tissue. Carbon is one of the four main elements building up human tissue and it is also an important component of "tissue-like" phantoms used for dose measurements. In the tissue-like materials carbon replaces the oxygen of real tissue, and therefore information for both nuclei is of importance to be able to convert the dose measured with phantoms to the dose in real tissue.

Neutron scattering measurements are often, due to experimental difficulties and limitations, restricted to the energy region below 15 MeV. Above that energy accurate data are very scarce. In recent years, however, a few facilities with high performance in the 20 MeV range have come into operation. Thus, the Ohio beam-swinger facility/1/ has been used to collect high precision data for several nuclei in the 20 - 26 MeV range. In Studsvik the high resolution time-of-flight facility/2/ has been used for a systematic study of elastic and inelastic neutron scattering at 21.6 MeV for 13 nuclei ranging from Magnesium to Bismuth/3/.

For carbon the Ohio group has measured elastic and inelastic scattering with high accuracy at four energies in the range 20.8 - 26 MeV /4,5/. However, there still exists a big gap between 15 and 20.8 MeV in the available data. We therefore found it worth-while to extend our measurements in order to fill this gap.

In this report a brief description of the experimental equipment and procedure will be given, as well as some experimental results and model calculations. Details of the full work can be found in ref. /6/.

Experimental apparatus and procedure

The present measurements were performed using the improved Studsvik fast neutron time-of-flight facility. The equipment and its application to neutron scattering in this energy region was extensively described in ref. /2/ and only a brief description will be given here.

The 5.5 MV CN Van de Graaff accelerator, equipped with two pulsing systems /7,8/, delivered 0.3 ns bursts of 1.5 - 5.5 MeV deuterons at a repetition rate of 1 MHz and with an average beam current of 3 μA. Monoenergetic neutrons at 16.5, 17.6, 18.7, 19.8, 20.9, 21.6 and 22.0 MeV were produced with the T(d,n) reaction, using a 1 or 2 cm long target cell filled with tritium gas to a pressure of up to 4 atm.

The carbon scattering sample consisted of a pure graphite hollow cylinder with natural isotopic composition (i.e. 98.9 % ^{12}C), having a height of 5.0 cm, an outer diameter of 2.5 cm, and an inner diameter of 1.0 cm. During measurements it was positioned at a distance of 14.5 cm in front of the gas target.

The detector system of the neutron time-of-flight spectrometer consisted of two 12.7 cm diameter by 5.1 cm thick NE 213 liquid scintillators directly coupled to fast 5" photomultiplier tubes. The detectors were separated by 5° and positioned at a distance of 3.5 - 4 m from the scattering sample in a heavy shielding consisting of iron, lead, and lithium-loaded paraffin. A Hevimet shadow bar ensured optimum attenuation of the direct target flux. The arrangement was placed on an arm, which could be moved on a horizontal circular track, with its axis in line with the scattering sample.

The total time resolution in the present experiment was measured to be 1 ns for elastic scattering at 22.0 MeV neutron energy, increasing to 2 ns at 16.5 MeV, corresponding to a total energy resolution of 0.8 and 1.0 MeV, respectively.

The spectra of scattered neutrons were measured in steps of 2.5° or 5° in the angular interval 10° - 160°. The background was observed without any sample in position at each angle and under identical experimental conditions to those used in the scattering measurements.

As an illustration of the experimen-

tal conditions a spectrum of neutrons emitted at 45° from the C + n reaction at 21.6 MeV is shown in fig. 1. Note that no background subtraction has been performed. As can be seen, the sample-out background is very small compared to the scattered yield over the entire energy region. Peaks corresponding to most of the excited levels up to 15 MeV in ^{12}C can be identified. The peaks near channels 160 and 280 arise from contaminant neutron groups.

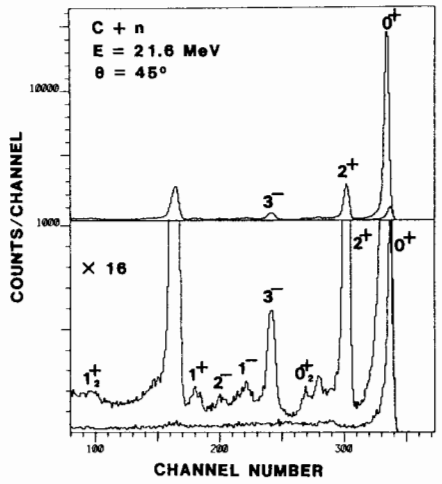

Fig. 1. Time-of-flight spectrum from the C + n reaction. The bottom part is a magnification by a factor of 16 of the upper part. The sample-out background has not been subtracted, but is indicated as the lower curve in the two parts.

The differential scattering cross sections were determined relative to the H(n,n)H cross section by observing the scattered yield from a parallelepipedic polyethylene sample with the dimensions 5.0 x 2.5 x 0.8 cm³ in the angular range 20° - 35°. Differential cross sections for the n-p scattering process were taken from the parameterization of Hopkins and Breit, using the Livermore (LRL CONSTRAINED) phase shifts/9/. The relative efficiency of the detectors as a function of energy was determined by measuring angular distributions of neutrons from the D(d,n) and T(d,n) reactions using thin, absorbed targets. To obtain information between these experimental points, they were normalized to a calculated efficiency curve/10/.

Neutron flux normalization was done by observing the source neutrons with a time-of-flight neutron monitor, housed in a collimating shielding positioned above the target at a distance of 4 m and at an angle of 80° with respect to the deuteron beam direction.

Corrections and experimental results

The finite neutron source-to-sample geometry used in the measurements necessitates the application of a number of corrections to the experimental data. Thus a small correction was applied for the anisotropic intensity ditribution of the target neutrons. Furthermore, the experimental elastic scattering data were corrected for neutron flux attenuation and multiple scattering in the sample as well as for the finite scattering geometry using an improved version of the Monte-Carlo code MULTSCAT 4 /11/. The inelastic scattering data were corrected for flux attenuation and for in- and out-scattering of neutrons to or from the state under consideration. Corrections for attenuation and multiple scattering in the polyethylene sample were carried out by applying the analytically expressed correction factor given in ref. /2/.

The total uncertainties in the measured differential cross sections are for elastic scattering generally in the range 3.6 - 10 % in the angular interval 10° - 160°, while for inelastic scattering they are typically in the range 5 - 20 %.

An example of the results for the fully corrected differential cross section data at 20.9 MeV are shown in fig. 2. The four data sets represent elastic scattering and inelastic scattering to the 4.44, 7.65 and 9.64 MeV levels, respectively. Shown are also the 20.8 MeV data from Ohio /4/, and as can be seen the agreement is excellent.

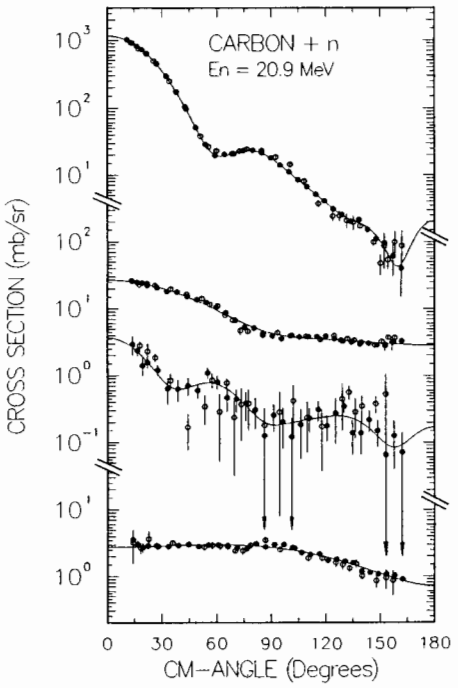

Fig. 2. Experimental differential cross sections for the scattering of 20.9 MeV neutrons by the ground- and first three excited states of ^{12}C (closed circles). Shown are also Legendre polynomial fits to the data (solid line) as well as the corresponding data at 20.8 MeV from Ohio /4/ (open circles).

Legendre polynomial expansions were fitted to the final, corrected differential elastic and inelastic scattering data. This representation provides a model-independent basis for obtaining the angle-integrated scattering cross sections and for extrapolating the angular distributions beyond the range of the measurements. The solid curves in fig. 2 are the results of such fits, and as can be seen the data are very well described. This holds also for the 7.65 MeV level, although the points show large statistical spread.

The angle integrated cross sections for elastic scattering are displayed in

fig. 3 together with the ENDF/B-V evaluation/12/ and some recent experimental data. In figs. 4 and 5 the corresponding results for the 4.44 and 9.64 MeV levels can be found. As can be seen the agreement with other recent data is generally very good. It is also obvious that the ENDF/B-V evaluation strongly underpredicts the cross sections above 15 MeV. The results for the 7.65 MeV level have been omitted in this report since its significance in bio-medical applications is negligible.

The differential cross sections for scattering from the ground state and the first excited state measured in this work are presented in fig. 6. The solid curves are the results of Legendre polynomial fits, while the dashed lines refer to model calculations, which will be described in the next section.

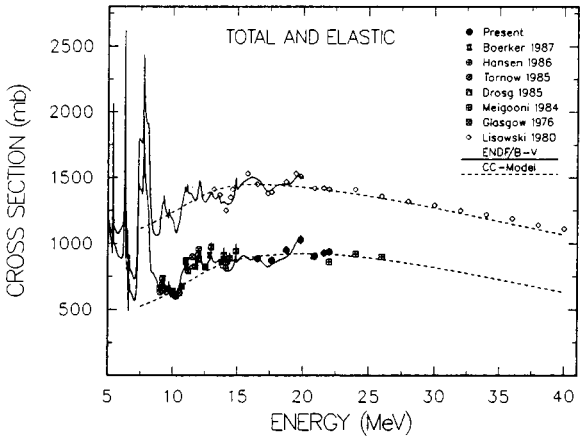

Fig. 3. Total and angle-integrated elastic cross sections for carbon versus energy. Shown are also data of refs. /4,13-17, 27/. The solid lines are the ENDF/B-V evaluation while the dashed lines are the results of the coupled-channels calculations.

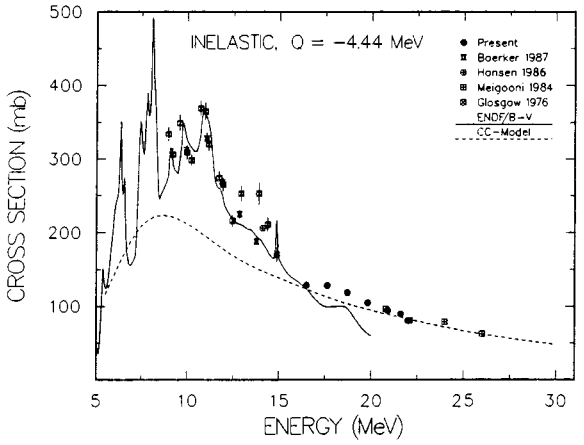

Fig. 4. Angle-integrated cross sections for the 4.44 MeV level of carbon versus energy. Shown are also data of refs. /4, 13-14,17/. The solid line is the ENDF/B-V evaluation while the dashed line is the result of the coupled-channels calculation.

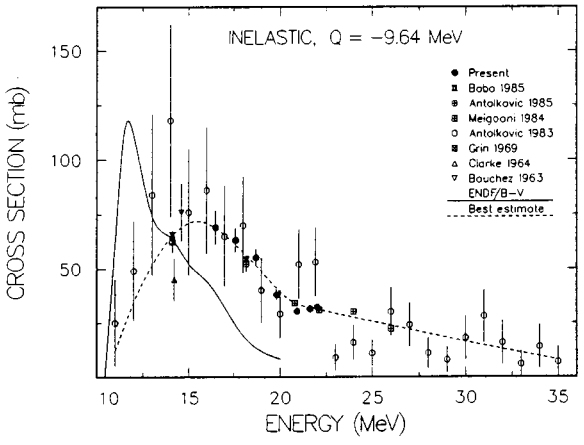

Fig. 5. Angle-integrated cross sections for the 9.64 MeV level of carbon versus energy. Shown are also data of refs. /4, 18-23/. The solid line is the ENDF/B-V evaluation while the dashed line is an estimate based on recent measurements.

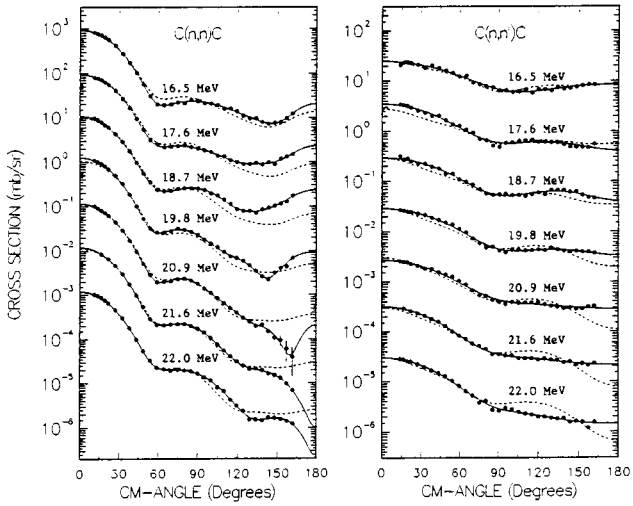

Fig. 6. Experimental differential cross sections for elastic and inelastic (4.44 MeV) scattering. For each higher energy the cross sections have been divided by 10. The solid lines are from the Legendre polynomial fits while the dashed lines are the results of the coupled-channels calculations.

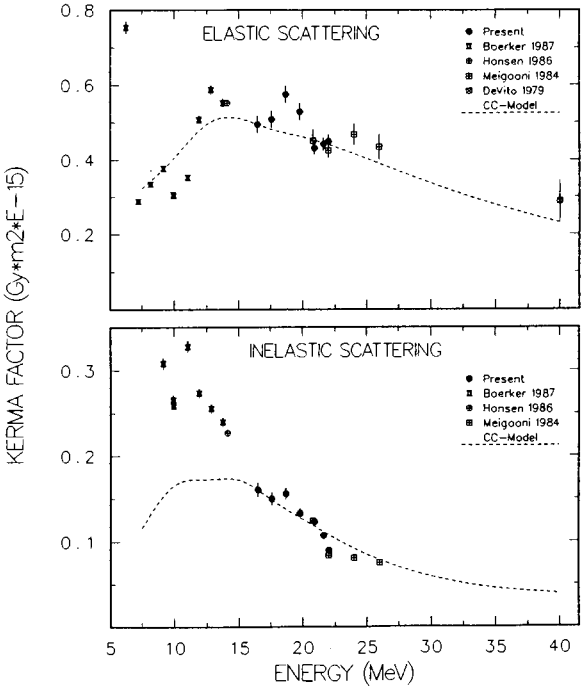

Fig. 7. Experimental kerma factors for elastic and inelastic (4.44 MeV) scattering versus energy. Shown are also data of refs. /4,13-14,25/. The dashed lines are the results from coupled-channels calculations.

Partial kerma factors for elastic and inelastic (4.44 MeV) scattering were calculated using the two first coefficients of the Legendre polynomial fits and the expressions of ref. /24/. The results are shown in fig. 7 together with some recent data, and as can be seen, the agreement is generally very good.

Coupled-channels calculations

It is obvious that a model with which the cross sections and kerma factors could be calculated both inside and outside the measured energy range would be of great value.

To find such a model we have analyzed the experimental data in terms of the coupled-channels formalism for rotational nuclei. In these calculations best fits to the elastic and inelastic (4.44 MeV) scattering data at each energy were determined with the ECIS79 code/26/. The parameters of the best fits were then used in an iterative procedure to find average geometries and energy dependent potential depths with which the data could be reasonably well described. The Ohio data/4/ were also included in order to give a more reliable energy dependence. The potential parameters resulting from this analysis are (with conventional notations):

$$V_R = 64.02 - 0.674\ E_n$$
$$r_R = 1.093, \quad a_R = 0.619$$

$$W_D = 1.16 + 0.251\ E_n$$
$$r_D = 1.319, \quad a_D = 0.327$$

$$\beta_2 = -0.65, \quad \beta_4 = 0.05$$

The spin-orbit part of the potential was considered to be spherical and were kept constant during the searches (ref. /4/: V = 6.2 MeV, r = 1.05 fm and a = 0.55 fm). In our calculations we found no evidence for the need of a volume absorption term, and consequently this term was put equal to zero. This would limit the model at higher energies.

The results of the calculations are shown as dashed curves in figs. 3, 4, 6 and 7. In fig. 3 the model has been used to calculate also the total cross section and as can be seen the agreement with the experimental data of ref. /27/ is very good up to 40 MeV. It is also clear that the model describes the average behaviour of the cross sections above 10 MeV quite well. The inelastic scattering, fig. 4, is nicely described above 15 MeV, whereas the model underpredicts the cross section below this energy. Compound nucleus effects may be the reason for this. The angular distributions of elastic and inelastic scattering shown in fig. 6 are reasonably described by the model. The deviations in the backward angles could be due to resonance effects in the compound nucleus. Also the partial kerma factors displayed in fig. 7 are quite well described above 15 MeV. For the elastic scattering the model calculations agree with the experimental points up to 40 MeV. In the case of inelastic scattering the model seems to underestimate the kerma factor below 15 MeV, just as was the case for the angle-integrated cross section.

In summary, the model described seems to be capable of reproducing both cross sections and kerma factors in the energy range 15 - 30 MeV quite well, and this conclusion may hold also up to 40 MeV.

REFERENCES

1. R.W. Finlay et al., Nucl. Instr. Meth. 198 (1982) 197.
2. N. Olsson and B. Trostell, Nucl. Instr. Meth. A245 (1986) 415.
3. N. Olsson et al., Nucl. Phys. A472 (1987) 237.
4. A.S. Meigooni, J.S. Petler and R.W. Finlay, Phys. Med. Biol. 29 (1984) 643.
5. A.S. Meigooni et al., Nucl. Phys. A445 (1985) 304.
6. N. Olsson, B. Trostell and E. Ramström, To be published.
7. P. Tykesson and T. Wiedling, Nucl. Instr. Meth. 77 (1970) 277.
8. N. Olsson, Nucl. Instr. Meth. 187 (1981) 341.
9. J.C. Hopkins and G. Breit, Nucl. Data Tables A9 (1971) 137.
10. R.A. Cecil, B.D. Anderson and R. Madey, Nucl. Instr. Meth. 161 (1979) 439.
11. B. Holmqvist, B. Gustavsson and T. Wiedling, Arkiv Fysik 34 (1967) 481.
12. "ENDF/B-V", evaluated by C.Y. Fu and F.G. Perey, Brookhaven National Laboratory (1977).
13. G. Börker et al., Contr. to 6th Symp. on Neutron Dosimetry, Neuherberg, Oct. 12-16, 1987.
14. L.F. Hansen, Preprint UCRL-95890 (1986), to be published.
15. W. Tornow et al., J. Phys. G: Nucl. Phys 11 (1985) 379.
16. M. Drosg et al., Contr. to the Int. Conf. on Nuclear Data for Basic and Applied Science, Santa Fe, New Mexico, May 13-17, 1985.
17. D.W. Glasgow et al., Nucl. Sci. Eng. 61 (1976) 521 (revised in 1982 by C.R. Gould).
18. M. Baba et al., Contr. to the Int. Conf. on Nuclear Data for Basic and Applied Science, Santa Fe, New Mexico, May 13-17, 1985.
19. B. Antolkovic, M. Turk and K. Kadija, Contr. to the Int. Conf. on Nuclear Data for Basic and Applied Science, Santa Fe, New Mexico, May 13-17, 1985.
20. B. Antolkovic et al., Nucl. Phys. A394 (1983) 87.
21. G.A. Grin et al., Helv. Phys. Acta 42 (1969) 990.
22. R.L. Clarke and W.G. Cross, Nucl. Phys. 53 (1964) 177.
23. R. Bouchez, J. Duclos and P. Perrin, Nucl. Phys. 43 (1963) 623.
24. R.S. Caswell, J.J. Coyne and M.L. Randolph, Rad. Res. 83 (1980) 217.
25. R.P. DeVito, PhD thesis, Michigan State Univ. (1979); Kerma factor calculated by ref. /4/.
26. ECIS79 code, written by J. Raynal, CEA, France.
27. P.W. Lisowski et al., Contr. to the Int. Conf. on Neutron Cross Sections for Technology, NBS Special Publication SP-594 524 (1980).